

Four-jet production via double parton scattering in pA collisions at the LHC

Boris Blok^{1,*} and Federico Alberto Ceccopieri^{1,2,†}

¹ *Department of Physics, Technion, Israel Institute of Technology, Haifa, 32000 Israel*

²*IFPA, Université de Liège, B4000, Liège, Belgium*

We present predictions for the double parton scattering (DPS) four-jet production cross sections in pA collisions at the LHC. Relying on the experimental capabilities to correlate centrality with impact parameter B of the proton-nucleus collision, we discuss a strategy to extract the double parton scattering contributions in pA collisions, which gives direct access to double parton distribution in the nucleon. We show that the production cross sections via DPS of four jets, out of which two may be light- or heavy-quark jets, are large enough to allow the method to be used already with data accumulated in 2016 pA run.

PACS numbers:

I. INTRODUCTION

The flux of incoming partons in hadron-induced reactions increases with the collision energy so that multiple parton interactions (MPI) take place, both in pp and pA collisions. The study of MPIs started in eighties in Tevatron era [1–3], both experimentally and theoretically. Recently a significant progress was achieved in the study of MPI, in particular of double parton scattering (DPS). From the theoretical point of view a new self consistent pQCD based formalism was developed both for pp [4–13] and pA DPS collisions [14] (see [15] for recent reviews). Recent observations of double open charm [16–19] and same sign WW ($ssWW$) production [20] clearly show the existence of DPS interactions in pp collisions.

The MPI interactions play a major role in the Underlying Event (UE) and thus are taken into account in all MC generators developed for the LHC [21, 22]. On the other hand the study of DPS will lead to understanding of two parton correlations in the nucleon. In particular the DPS cross sections involve new non-perturbative two-body quantities, the so-called two particle Generalised Parton Distribution Functions ($_2$ GPDs), which encode novel features of the non-perturbative nucleon structure. Such distributions have the potential to unveil two-parton correlations in the nucleon structure [23, 24] and to give access to information complementary to the one obtained from nucleon one-body distributions.

The study of MPI and in particular of the DPS reactions in pA collisions is important for our understanding of MPI in pp collisions and it constitutes a benchmark of the theoretical formalism available for these processes. On the other hand the MPI in pA collisions may play an important role in underlying event (UE) and high multiplicity events in pA collisions. Moreover it was argued in Ref. [14] that they are directly related to longitudinal parton correlations in the nucleon.

The theory of MPI and in particular DPS in pA collisions was first developed in [25], where it was shown that there are two DPS contributions at work in such a case. First, there is the so-called DPS1 contribution, depicted in the left panel of Fig. (1), in which two partons from the incoming nucleon interact with two partons in the target nucleon in the nucleus, making such a process formally identical to DPS in the pp collisions. Next there is a new type of contribution, depicted in

*Electronic address: blok@physics.technion.ac.il

†Electronic address: federico.ceccopieri@hotmail.it

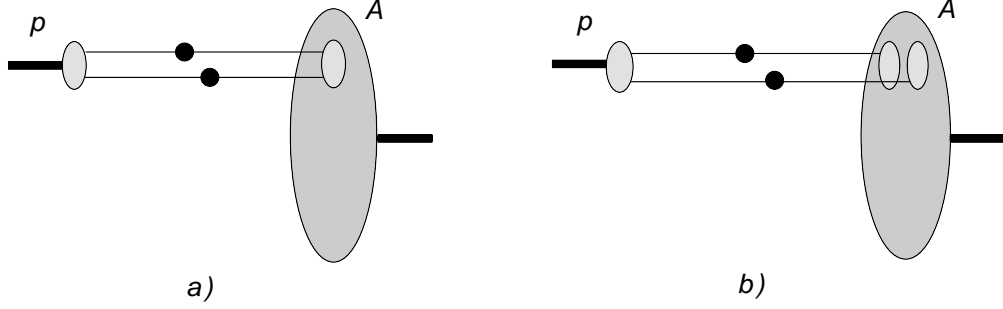


FIG. 1: Pictorial representation of DPS process in pA collisions via a) DPS1 and b) DPS2 mechanisms. The light grey blobs indicate nucleons, darker grey ones the nucleus and black ones the hard interactions.

the right panel of Fig. (1) and often called DPS2, in which two partons from the incoming nucleon interact with two partons each of them belonging to the distinct nucleons in the target nucleus located at the same impact parameter. Such a contribution is parametrically enhanced by a factor $A^{1/3}$ over the DPS1 contribution, A being the atomic number of the nucleus.

In the recent past a number of theoretical studies have appeared which focus on the study of DPS contributions in pA collisions [14, 26–30]. However, although many interesting theoretical studies of DPS2 were performed recently, the problem remains is how to observe DPS2 experimentally. The main issue is obviously the large SPS (leading twist) background in such processes, that makes the observation of the DPS contributions, which are next to leading twist phenomena, a rather complicated task.

Recently however a new method was suggested in Ref. [31], which allows to separate DPS2 from the leading twist (and DPS1) contributions. The method exploits the different dependence on the impact parameter B on the various contributions to pA cross section for a given final state: while the SPS and DPS1 contributions are proportional to the nuclear thickness function $T(B)$, the DPS2 one is proportional to the square of $T(B)$. Therefore the cross section producing a given final state can be schematically written as [31],:

$$\frac{d^2\sigma_{pA}}{d^2B} = \left(\sigma_{pA}^{LT} + \sigma_{pA}^{DPS1}\right) \frac{T(B)}{A} + \sigma_{pA}^{DPS2} \frac{T^2(B)}{\int d^2B T^2(B)}, \quad (1)$$

where $T(B)$ is normalized to the atomic number A of the nucleus. This approach was used in Ref. [31] to study two-dijets processes and, in Ref. [32], to study processes involving the associated production of electroweak bosons and jets in pA collisions.

The latter strategy exploits the experimental capabilities to accurately relate centrality with the impact parameter B of the pA collisions. The procedure for the determination of centrality in pA collisions was developed i.e. by ATLAS [33]. It makes use of the measurement of the transverse energy E_T deposited in the pseudorapidity interval $-3.2 \geq \eta \geq -4.9$ (i.e. along the nucleus direction) as a measure of centrality. It was shown in Ref. [34] that E_T in this kinematics is not sensitive to production of hadrons at forward rapidities. The E_T distribution as a function of the number of collisions ν (and thus on the impact parameter B) is presented in Refs. [33–35] (see also the related discussion in Ref. [31]).

The purpose of the present paper is to continue the research started in those works and pursue the emergence of DPS2 contribution in the four-jet final state. Indeed, the observation of DPS in pA collisions faces two main challenges: the first one, in common with DPS studies in pp collisions, is tackling the large single parton scattering (SPS) background; the second one is given by the limited integrated luminosity accumulated in short pA runs, which is several orders of magnitude integrated lower than the one accumulated in pp collisions. Therefore the obvious question is

whether the number of observed DPS events is sufficient to overcome the systematic inaccuracy due to the large SPS background. Such question was studied for example in [32] where we found that it is possible to separate SPS and DPS2 backgrounds for Wjj final state.

The purpose of this paper is to investigate the possibility to isolate the DPS2 contribution within multi-jet final state and the necessary kinematic constraints. We shall calculate the cross sections as a function of impact parameter B of the pA collision, for its various components in both the four-jet ($4j$) and two b -jet plus two light jets ($2b2j$) final states and estimate the sensitivity to the DPS mechanisms for the considered final states. We shall see, that both these final states are the "golden plate" channel for the observation of the DPS2 mechanism.

The paper is organised as follows. In Section II we review the theoretical formalism and the set up for our calculations. In Sec. III and IV we analyze and discuss the results in the $4j$ and $2b2j$ final states, respectively. We summarize our results in conclusion.

II. THEORETICAL FRAMEWORK

The cross section for the production of final states C and D in pA collisions via double parton scattering can be written as the convolution of the double $_2\text{GPDs}$ of the proton and the nucleus, G_p and G_A , respectively [14, 25]:

$$\frac{d\sigma_{DPS}^{CD}}{d\Omega_C d\Omega_D} = \int \frac{d^2\vec{\Delta}}{(2\pi)^2} \frac{d\hat{\sigma}_{ik}^C(x_1, x_3)}{d\Omega_C} \frac{d\hat{\sigma}_{jl}^D(x_2, x_4)}{d\Omega_D} G_p^{ij}(x_1, x_2, \vec{\Delta}) G_A^{kl}(x_3, x_4, -\vec{\Delta}). \quad (2)$$

Two parton GPDs depend on the transverse momentum imbalance momentum $\vec{\Delta}$. The structure and relative weight of different contributions to the nuclei $_2\text{GPD}$ was studied in detail in Ref. [14], where it was shown that only two contributions survive: the one that corresponds to DPS1 mechanism and an other corresponding to DPS2.

Since our analysis will especially deal with impact parameter B dependence of the cross section, we find natural to rewrite Eq. (2) in coordinate space, introducing the double distributions $D_{p,A}$ which are the Fourier conjugated of $G_{p,A}$ with respect to $\vec{\Delta}$. In such a representation these distributions admit a probabilistic interpretation and represent the number density of parton pairs with longitudinal fractional momenta x_1, x_2 , at a relative transverse distance \vec{b}_\perp , the latter being the Fourier conjugated to $\vec{\Delta}$.

In the impulse approximation for the nuclei, neglecting possible corrections to factorisation due to the shadowing for large nuclei, and taking into account that $R_A \gg R_p$ for heavy nuclei, we can rewrite the cross section as [14, 25]

$$\begin{aligned} \frac{d\sigma_{DPS}^{CD}}{d\Omega_1 d\Omega_2} &= \frac{m}{2} \sum_{i,j,k,l} \sum_{N=p,n} \int d\vec{b}_\perp \int d^2B D_p^{ij}(x_1, x_2; \vec{b}_\perp) D_N^{kl}(x_3, x_4; \vec{b}_\perp) T_N(B) \frac{d\hat{\sigma}_{ik}^C}{d\Omega_C} \frac{d\hat{\sigma}_{jl}^D}{d\Omega_D}, \\ &+ \frac{m}{2} \sum_{i,j,k,l} \sum_{N_3, N_4=p,n} \int d\vec{b}_\perp D_p^{ij}(x_1, x_2; \vec{b}_\perp) \int d^2B f_{N_3}^k(x_3) f_{N_4}^l(x_4) T_{N_3}(B) T_{N_4}(B) \frac{d\hat{\sigma}_{ik}^C}{d\Omega_C} \frac{d\hat{\sigma}_{jl}^D}{d\Omega_D}. \end{aligned} \quad (3)$$

Here $m = 1$ if C and D are identical final states and $m = 2$ otherwise, $i, j, k, l = \{q, \bar{q}, g\}$ are the parton species contributing to the final states $C(D)$. In Eq. (3) and in the following, $d\hat{\sigma}$ indicates the partonic cross section for producing the final state $C(D)$, differential in the relevant set of variables, Ω_C and Ω_D , respectively. The functions f^i appearing in Eq. (3) are single parton densities and the subscript N indicates nuclear parton distributions. The double parton diistribution D_N is the double GPD for the nucleon bound in the nuclei, once again calculated in the mean field approximation.

Partonic cross sections and parton densities do additionally depend on factorization and renormalization scales whose values are set to appropriate combination of the large scales occurring in final state C and D .

The nuclear thickness function $T_{p,n}(B)$, mentioned in the Introduction and appearing in Eq. (3), is obtained integrating the proton and neutron densities $\rho_0^{(p,n)}$ in the nucleus over the longitudinal component z

$$T_{p,n}(B) = \int dz \rho^{(p,n)}(B, z), \quad (4)$$

where we have defined r , the distance of a given nucleon from nucleus center, in terms of the impact parameter B between the colliding proton and nucleus, $r = \sqrt{B^2 + z^2}$. Following Ref. [36], for the ^{208}Pb nucleus, the density of proton and neutron is described by a Wood-Saxon distribution

$$\rho^{(p,n)}(r) = \frac{\rho_0^{(p,n)}}{1 + e^{(r-R_0^{(p,n)})/a_{(p,n)}}}. \quad (5)$$

For the neutron density we use $R_0^n = 6.7$ fm and $a_n = 0.55$ fm [37]. For the proton density we use $R_0^p = 6.68$ fm and $a_p = 0.447$ fm [38]. The $\rho_0^{(p,n)}$ parameters are fixed by requiring that the proton and neutron density, integrated over all distance r , are normalized to the number of the protons and neutrons in the lead nucleus, respectively.

As already anticipated, the DPS1 contribution, the first term in Eq. (3), stands for the contribution already at work in pp collisions. It depends linearly on the nuclear thickness function T and therefore scales as the number of nucleon in the nucleus, A .

The second term, the DPS2 contribution, contains in principle two-body nuclear distributions. We work here in the impulse approximation, neglecting short range correlations in the nuclei since their contribution may change the results by several percent only [31]. The latter term is therefore proportional to the product of one-body nucleonic densities in the nucleus, *i.e.* it depends quadratically on T and parametrically scales as $A^{4/3}$.

As we already stated above we shall work here for simplicity in the mean field approximation for the nucleon. In such approximation double GPD has a factorized form :

$$D_p^{ij}(x_1, x_2, \mu_A, \mu_B, \vec{b}_\perp) \simeq f_p^i(x_1, \mu_A) f_p^j(x_2, \mu_B) \mathcal{T}(\vec{b}_\perp), \quad (6)$$

where the function $\mathcal{T}(\vec{b}_\perp)$ describes the probability to find two partons at a relative transverse distance \vec{b}_\perp in the nucleon and is normalized to unity. In such a simple approximation, this function does not depend on parton flavour and fractional momenta. Then one may define the so-called effective cross section as

$$\sigma_{eff}^{-1} = \int d\vec{b}_\perp [\mathcal{T}(\vec{b}_\perp)]^2, \quad (7)$$

which controls the double parton interaction rate. Under all these approximations the DPS cross section in pA collision can be rewritten as

$$\begin{aligned} \frac{d\sigma_{DPS}^{CD}}{d\Omega_1 d\Omega_2} &= \frac{m}{2} \sum_{i,j,k,l} \sum_{N=p,n} \sigma_{eff}^{-1} f_p^i(x_1) f_p^j(x_2) f_N^k(x_3) f_N^l(x_4) \frac{d\hat{\sigma}_{ik}^C}{d\Omega_C} \frac{d\hat{\sigma}_{jl}^D}{d\Omega_D} \int d^2 B T_N(B), \\ &+ \frac{m}{2} \sum_{i,j,k,l} \sum_{N_3, N_4=p,n} f_p^i(x_1) f_p^j(x_2) f_{N_3}^k(x_3) f_{N_4}^l(x_4) \frac{d\hat{\sigma}_{ik}^C}{d\Omega_C} \frac{d\hat{\sigma}_{jl}^D}{d\Omega_D} \int d^2 B T_{N_3}(B) T_{N_4}(B). \end{aligned} \quad (8)$$

Ref.	selection	$\sigma_{eff}[mb]$
[45]	$N_{jets} \geq 4, p_T^j \geq 20 \text{ GeV}, \eta_j \leq 4.4$ and at least one having $p_T \geq 42.5 \text{ GeV}$	$14.9^{+1.2}_{-1.0}(stat.)^{+5.1}_{-3.8}(syst.)$
[43]	$N_{jets} = 4$: two jets with $p_T \geq 50 \text{ GeV}$ two jets with $p_T \geq 20 \text{ GeV}, \eta_j \leq 4.7$	$19.0^{+4.6}_{-3.0}$ [46]
[44]	two light jets and two b -jets with $p_T \geq 20 \text{ GeV}$ $ \eta_b \leq 2.4, \eta_j \leq 4.7$	$23.3^{+3.3}_{-2.5}$ [46]

TABLE I: Kinematic selection for the $4j$ and $2b2j$ final states adopted in experimental analyses and the corresponding values of extracted σ_{eff} .

We find important to remark the key observation that leads to the second term of Eq. (3): namely that the b and B integrals practically decouple since the nuclear density does not vary on subnuclear scale [14, 25, 29]. As a result this term does depend on ${}_2\text{GPDs}$ integrated over transverse distance b_\perp , i.e. at $\vec{\Delta} = 0$, for which we assume again mean field approximation:

$$\int d\vec{b}_\perp D_p^{ij}(x_1, x_2; \vec{b}_\perp) \simeq f_p^i(x_1) f_p^j(x_2). \quad (9)$$

After integration over b_\perp in Eq. (7), σ_{eff} will be the only non-perturbative parameter characterising the DPS1 cross section. We use in our calculation σ_{eff} values extracted from experimental analyses of DPS processes in pp collisions. We neglect corrections due to longitudinal correlations in the nucleon [14] and any possible dependence of σ_{eff} on energy [39]. For the considered final state a number of experimental analyses have extracted its values for pp collisions at $\sqrt{s}=7 \text{ TeV}$ which are reported in the Tab. (I). In our numerical estimates we use the average of those values, $\bar{\sigma}_{eff} = 19 \text{ mb}$.

We close this Section by specifying the kinematics and additional settings with which we evaluate Eq. (8). We consider proton lead collisions at a centre-of-mass energy $\sqrt{s_{pN}} = 8.16 \text{ TeV}$. Due to the different energies of the proton and lead beams ($E_p = 6.5 \text{ TeV}$ and $E_{Pb} = 2.56 \text{ TeV}$ per nucleon), the resulting proton-nucleon centre-of-mass is boosted with respect to the laboratory frame by $\Delta y = 1/2 \ln E_p/E_N = 0.465$ in the proton direction, assumed to be at positive rapidity. Therefore jets rapidities, in this frame, are given by $y_{CM} = y_{lab} - \Delta y$. All calculations are based on proton-nucleon centre-of-mass rapidities.

All the relevant DPS and SPS cross sections contributing to the $4j$ and $2b2j$ final states have been calculated to leading order with ALPGEN [40]. Jet cross sections are obtained by identifying final state partons as jets, as appropriate for a leading order calculations.

We use CTEQ6L1 leading order free proton parton distributions [41]. Nuclear effects on the cross sections are estimated by using EPS09 nuclear parton distributions [42] in separate simulations. They are found to reduce the dijet cross sections less than 1% for $p_T^j > 20 \text{ GeV}$ and are neglected. We also mention that dijet cross sections are, to very good accuracy, the same on target protons or neutrons, so no isospin corrections is applied.

III. RESULTS : $4j$

In this Section we present results for the inclusive production of, at least, four light jets. Two leading jets are requested to have $p_T^{j1,j2} > 50 \text{ GeV}$, the subleading ones $p_T^{j3,j4} > 20 \text{ GeV}$ and

	DPS1	DPS2	SPS	Sum	$\sigma(4j)/\sigma(2j)$	f_{DPS1}	f_{DPS2}
$4j$	$[\mu\text{b}]$	$[\mu\text{b}]$	$[\mu\text{b}]$	$[\mu\text{b}]$			
$p_T^{j_3,j_4} > 20 \text{ GeV}$	26.0	72.2	170.9	269.2	0.15	0.13	0.27
$p_T^{j_3,j_4} > 25 \text{ GeV}$	10.8	30.2	92.9	133.9	0.07	0.10	0.22
$p_T^{j_3,j_4} > 30 \text{ GeV}$	5.1	14.3	51.4	70.9	0.04	0.09	0.20

TABLE II: Predictions for $4j$ DPS and SPS cross sections in pA collisions in fiducial phase space, for different cuts on jets transverse momenta.

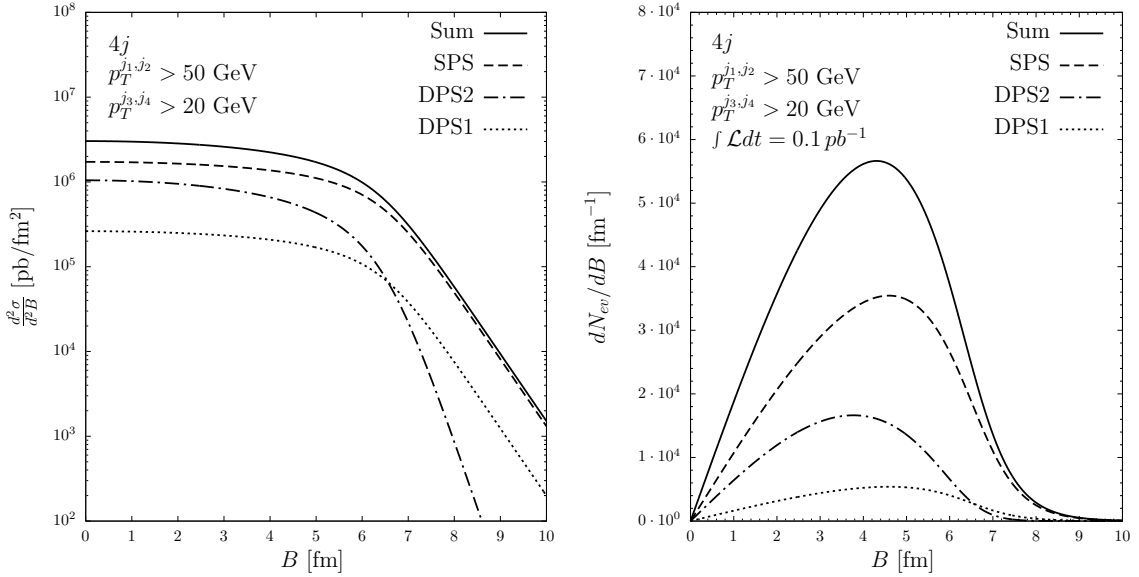


FIG. 2: Differential cross section as a function of B for the various contributions to the $4j$ final state (left). Expected number of events for the various contributions assuming $\int \mathcal{L} dt = 0.1 \text{ pb}^{-1}$ (right).

$|y_j^{lab}| < 4.7$. Different cuts on the leading and subleading jets are enforced to facilitate the pairing for the DPS selection. Both for the DPS and the SPS mechanisms we require the interparton distance in the $\eta - \phi$ plane

$$\Delta R_{ij} = \sqrt{(\eta_i - \eta_j)^2 + (\phi_i - \phi_j)^2} \quad (10)$$

to be $\Delta R_{ij} > 0.7$, where i and j stands for a generic light jets ($i, j = 1 \dots 4, i \neq j$). In the DPS cross section we set the symmetry factor $m = 2$ when the subleading jets have $20 < p_T^{j_3,j_4} < 50 \text{ GeV}$ and $m = 1$ if $p_T^{j_3,j_4} > 50 \text{ GeV}$. The factorization and renormalization scales are fixed to $\mu_F = \mu_R = \sqrt{\sum_j^{N_{jet}} p_{T,j}^2}$, where $N_{jet} = 2$ in DPS and $N_{jet} = 4$ in SPS. All the calculations are performed with ALPGEN [40].

We report in Tab. II the various contributions to the $4j$ fiducial cross section for three different transverse momentum cuts on the subleading jets. In the last three columns we report the ratio between the 4 jets (SPS+DPS) over 2 jets (with $p_T > 50 \text{ GeV}$) cross section, the DPS1 fraction f_{DPS1} calculated as DPS1 over (DPS1+SPS) cross section (for easy reference to pp collisions) and the DPS2 fraction f_{DPS2} , calculated as DPS2 over (DPS1+DPS2+SPS) cross section. In general we observe a large contributions from DPS2, which reaches 27% of 4 jets cross section for $p_T^{j_3,j_4} >$

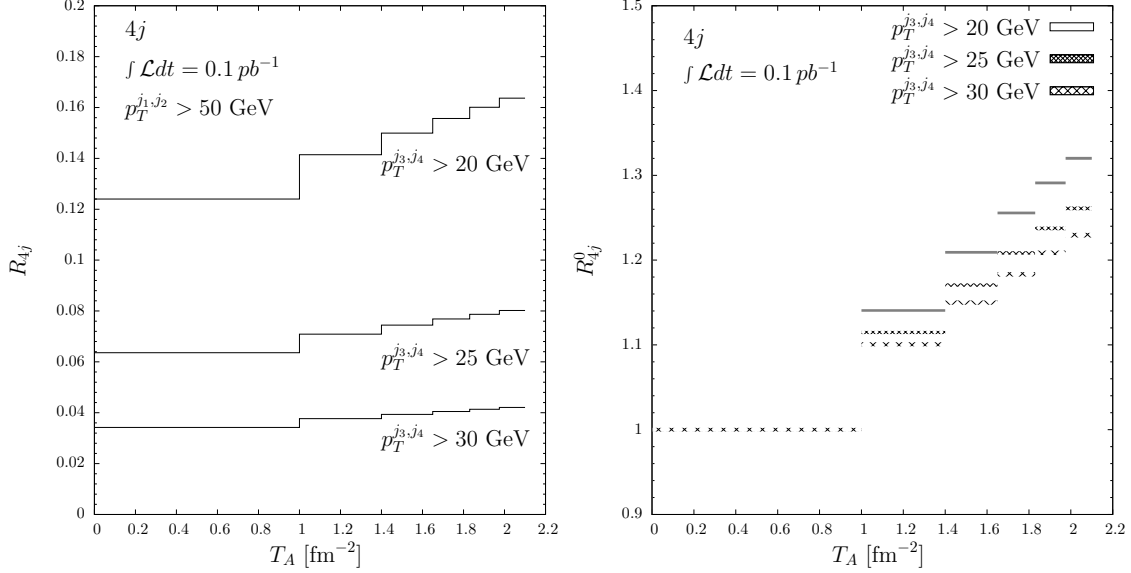


FIG. 3: The ratio in Eq. (12) (left) and double ratio in Eq. (13) (right) integrated in bins of $T_A(B)$. Predictions are shown for three different cuts on jet transverse momenta.

20 GeV. We present in the left panel of Fig. (2) the various contributions to the cross sections differential in B and the right panel the expected number of events assuming $\int \mathcal{L}dt = 0.1 \text{ pb}^{-1}$, a value in line with data recorded in 2016 pA runs. Exploiting the different dependence on T of the various contributions, we may use the strategy put forward in Ref. [31] to separate the DPS2 contribution. For this purpose we evaluate the number of events integrating Eq. (1) in the i -bin specified by the the bin-edge values T_i and T_{i+1} :

$$N_{ev}(T_i, T_{i+1}) = \int d^2B \frac{d^2\sigma_{pA}}{d^2B} \Theta(T_A(B) - T_i) \Theta(T_{i+1} - T_A(B)) \quad (11)$$

and then we consider the ratio R_{4j} between the total number (DPS+SPS) of $4jets$ events over those for dijet production (with $p_T > 50 \text{ GeV}$) as a function of $T_A(B)$:

$$R_{4j}(T_i, T_{i+1}) = N_{4j}(T_i, T_{i+1})/N_{2j}(T_i, T_{i+1}). \quad (12)$$

In such a ratio, N_{2j} is linear in $T_A(B)$, as well as the SPS background and the DPS1 mechanisms which both contribute to N_{4j} . In absence of the quadratic DPS2 contribution, such a ratio would be a constant. Its presence, on the other hand, will induce a linear increase of the ratio as a function of T , and the DPS2 magnitudo will determine its slope.

The resulting distribution is presented in the left panel of Fig. (3) for different values of jet transverse momenta cut off and integrated in bins of T , chosen to evenly distribute the number of events. The rise of the slope is related to fast rise of the dijet cross sections entering the DPS2 estimation as the cuts on jet transverse momenta are decreased. Our calculations were done to the LO (Leading Order) in strong coupling. Therefore it is natural to ask for the stability of the ratio in Eq. (12). The role of higher order corrections for the $4j$ final state has been investigated in a number of papers and corrections has been found to be large [47, 48]. In order to partially overcome this problem, we form double ratio

$$R_{4j}^0(T_i, T_{i+1}) = \frac{N_{4j}(T_i, T_{i+1})}{N_{2j}(T_i, T_{i+1})} \left(\frac{N_{4j}(T_0, T_1)}{N_{2j}(T_0, T_1)} \right)^{-1} \quad (13)$$

	DPS1	DPS2	SPS	Sum	$\sigma(2b2j)/\sigma(2j)$	f_{DPS1}	f_{DPS2}
$2b2j$	$[\mu\text{b}]$	$[\mu\text{b}]$	$[\mu\text{b}]$	$[\mu\text{b}]$	$\cdot 10^{-4}$		
$p_T^{b,j} > 20 \text{ GeV}$	2.2	6.2	13.0	21.4	3.0	0.15	0.29
$p_T^{b,j} > 25 \text{ GeV}$	0.4	1.2	4.7	6.4	2.1	0.09	0.19
$p_T^{b,j} > 30 \text{ GeV}$	0.1	0.3	1.9	2.3	1.6	0.06	0.13

TABLE III: Predictions for $2b2j$ DPS and SPS cross sections in pA collisions in fiducial phase space for different cuts on jets transverse momenta.

i.e. we normalize it to the first bin with $T_0 = 0 \text{ fm}^{-2}$ and $T_1 = 1 \text{ fm}^{-2}$. The resulting distribution is presented in the right panel of Fig. (3). Assuming that statistical errors follow a Poissonian distribution, the associated error is derived from the expected number of events. Our results indicate that, within these errors estimates, the departure from a constant behaviour can be unambiguously appreciated and the DPS2 contribution disentangled already from data of 2016 pA runs, modulo the experimental issues in studying the most peripheral events.

IV. RESULTS : $2b2j$

We consider in this Section a special class of the former process in which the second scattering produces a $b\bar{b}$ heavy-quark pair. Experimental results for this final state are reported in Ref. [44]. Light and heavy quarks jet are all requested to have $p_T > 20 \text{ GeV}$. Additionally light jet are requested to have $|\eta_j^{ab}| < 4.7$ and heavy quarks jets $|\eta_b^{ab}| < 2.4$. For this final state, the symmetry factor in the DPS cross sections is set to $m = 2$. The additional heavy quark tagging facilitate the pairing in the DPS selection. Both for DPS and SPS mechanisms we set $\Delta R_{ij} > 0.7$ where both index runs over light and heavy quarks jets. The factorization and renormalization scales are fixed to $\mu_F = \mu_R = \sqrt{\sum_j^{N_{jet}} m_{T,j}^2}$, where $N_{jet} = 2$ in DPS and $N_{jet} = 4$ in SPS, being $m_{T,j} = \sqrt{m_j^2 + p_{T,j}^2}$, the transverse mass of jet j . All the calculations are performed with ALPGEN [40].

We report in Tab. III the various contributions to the $2b2j$ fiducial cross section for three different transverse momentum cuts on the jets. In general we observe a large contributions from DPS2, which reaches 29% for $p_T > 20 \text{ GeV}$. We present in the left panel of Fig. (4) the various contributions to the cross sections differential in B and the right panel the expected number of events assuming $\int \mathcal{L} dt = 0.1 \text{ pb}^{-1}$. As in the previous Section, we consider the ratio R_{2b2j} between the total number of $2b2j$ events (DPS+SPS) over those for dijet production as a function of $T_A(B)$:

$$R_{2b2j}(T_i, T_{i+1}) = N_{2b2j}(T_i, T_{i+1})/N_{2j}(T_i, T_{i+1}). \quad (14)$$

The resulting distribution is presented in the left panel of Fig. (5) for different values of jet transverse momenta cut off and integrated in bins of T . The rise of the slope is related to fast rise of the dijet cross sections entering the DPS2 estimation as the cuts on jet transverse momenta are decreased. As shown in Tab.(3) of Ref. [44], the comparison of various theoretical predictions with $2b2j$ data reveal substantial agreement with NLO predictions but LO prediction suffers from large higher order corrections. Such a results are confirmed also by ALPGEN prediction which returns a cross section 0.6 times smaller than data [44]. In order to partly mitigate these effects, we form

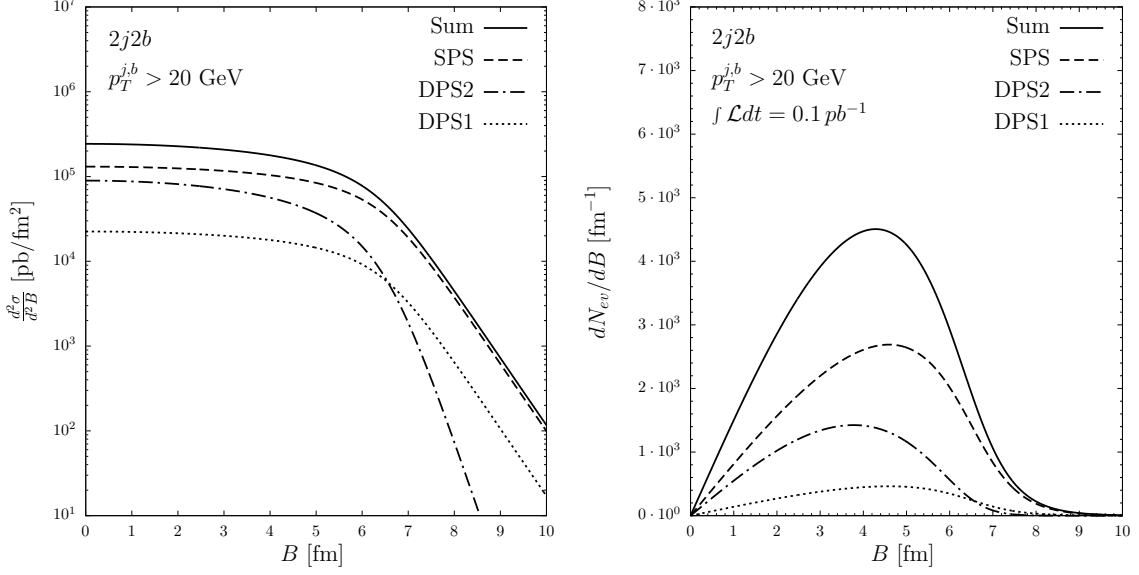


FIG. 4: Differential cross section as a function of B for the various contributions to the $2b2j$ final state (left). Expected number of events for the various contributions assuming $\int \mathcal{L} dt = 0.1 \text{ pb}^{-1}$ (right).

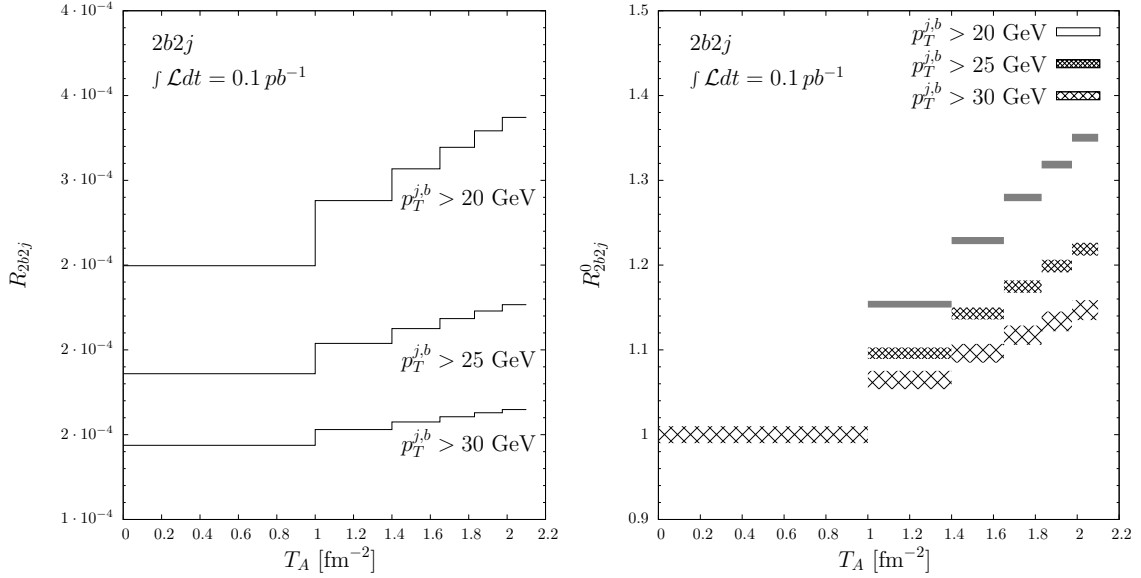


FIG. 5: The ratio in Eq. (14) (left panel) and double ratio in Eq. (15) (right panel) integrated in bins of $T_A(B)$. Predictions are shown for three different cuts on jet transverse momenta.

the double ratio

$$R_{2b2j}^0(T_i, T_{i+1}) = \frac{N_{2b2j}(T_i, T_{i+1})}{N_{2j}(T_i, T_{i+1})} \left(\frac{N_{2b2j}(T_0, T_1)}{N_{2j}(T_0, T_1)} \right)^{-1} \quad (15)$$

i.e. we normalize it to the first bin ($0 < T < 1$). The resulting distribution is presented in the right panel of Fig. (5). The associated error is calculated from the expected number of events, assuming a Poissonian distribution for statistical errors.

Our results indicate that, although with lesser significance with respect to the four-jet case, the departure from a constant behaviour can be unambiguously observed also in this final state.

As already observed in the $4j$ case, lowering the cut on the jet transverse momenta increases the sensitivity to a non constant behaviour of R_{2b2j}^0 .

V. CONCLUSIONS

In this paper we have calculated DPS cross sections for double dijet final states produced in pA collisions at the LHC, as well as the corresponding SPS backgrounds. Relying on the experimental capabilities to correlate centrality with impact parameter B of the proton-nucleus collision, we have presented a strategy to extract the so-called DPS2 contributions, pertinent to pA collisions. With this respect the $4j$ and $2b2j$ final states has large enough cross sections to allow the use of the method [31] to disentangle Leading Twist + DPS1 contributions from the DPS2 contribution, which is the main interest of this paper, already with data accumulated in 2016 pA run.

Acknowledgments

The authors would like to thank M. Strikman for reading the manuscript and for many useful discussions. We also thank A. Milov for many useful comments. The work was supported by Israel Science Foundation under the grant 2025311. The diagram in this paper has been drawn with Jaxodraw package version 2.0 [49].

-
- [1] N. Paver and D. Treleani, *Nuovo Cim. A* **70** (1982) 215.
 - [2] N. Paver and D. Treleani, *Phys. Lett.* **146B** (1984) 252.
 - [3] M. Mekhfi, *Phys. Rev. D* **32** (1985) 2371.
 - [4] J.R. Gaunt and W.J. Stirling, *JHEP* **1003**, 005 (2010)
 - [5] B. Blok, Yu. Dokshitzer, L. Frankfurt and M. Strikman, *Phys. Rev. D* **83**, 071501 (2011)
 - [6] M. Diehl, *PoS D* **IS2010** (2010) 223
 - [7] J.R. Gaunt and W.J. Stirling, *JHEP* **1106**, 048 (2011)
 - [8] B. Blok, Yu. Dokshitzer, L. Frankfurt and M. Strikman, *Eur. Phys. J. C* **72**, 1963 (2012)
 - [9] M. Diehl, D. Ostermeier and A. Schafer, *JHEP* **1203** (2012) 089
 - [10] B. Blok, Yu. Dokshitzer, L. Frankfurt and M. Strikman, *arXiv:1206.5594v1 [hep-ph]* (unpublished).
 - [11] B. Blok, Y. Dokshitzer, L. Frankfurt and M. Strikman, *Eur. Phys. J. C* **74** (2014) 2926
 - [12] M. Diehl, J. R. Gaunt and K. Schönwald, *JHEP* **1706** (2017) 083
 - [13] A. V. Manohar and W. J. Waalewijn, *Phys. Rev. D* **85** (2012) 114009
 - [14] B. Blok, M. Strikman and U. A. Wiedemann, *Eur. Phys. J. C* **73** (2013) no.6, 2433
 - [15] *Adv. Ser. Direct. High Energy Phys.* **29** (2018) 2019, P. Bartalini and J. Gaunt Editors.
 - [16] I. M. Belyaev, talk at MPI-2015 conference.
 - [17] R. Aaij *et al.* [LHCb Collaboration], *JHEP*, 1206 (2012) 141; Addendum 1403 (2014) 108
 - [18] R. Aaij *et al.* [LHCb Collaboration], *Nucl. Phys. B* **871** (2013) 1.
 - [19] R. Aaij *et al.* [LHCb Collaboration], *JHEP* **1607** (2016) 052
 - [20] A. M. Sirunyan *et al.* [CMS Collaboration], *Eur. Phys. J. C* **80** (2020) no.1, 41
 - [21] T. Sjöstrand *et al.*, *Comput. Phys. Commun.* **191** (2015) 159
 - [22] M. Bahr *et al.*, *Eur. Phys. J. C* **58** (2008) 639
 - [23] G. Calucci and D. Treleani, *Phys. Rev.* **D60**, 054023 (1999).
 - [24] M. Rinaldi and F. A. Ceccopieri, *Phys. Rev. D* **97** (2018) no.7, 071501
 - [25] M. Strikman and D. Treleani, *Phys. Rev. Lett.* **88** (2002) 031801
 - [26] I. Helenius and H. Paukkunen, *Phys. Lett. B* **800** (2020) 135084
 - [27] D. d'Enterria and A. Snigirev, *Adv. Ser. Direct. High Energy Phys.* **29** (2018) 159
 - [28] E. Cattaruzza, A. Del Fabbro and D. Treleani, *Phys. Rev. D* **70** (2004) 034022
 - [29] S. Salvini, D. Treleani and G. Calucci, *Phys. Rev. D* **89** (2014) no.1, 016020

- [30] O. Fedkevych and L. Lönnblad, arXiv:1912.08733 [hep-ph].
- [31] M. Alvioli, M. Azarkin, B. Blok and M. Strikman, Eur. Phys. J. C **79** (2019) no.6, 482
- [32] B. Blok and F. A. Ceccopieri, arXiv:1912.02508 [hep-ph]. to be published in European Journal of Particle Physics (EPJC).
- [33] G. Aad *et al.* [ATLAS Collaboration], Eur. Phys. J. C **76** (2016) no.4, 199
- [34] G. Aad *et al.* [ATLAS Collaboration], Phys. Lett. B **756** (2016) 10
- [35] G. Aad *et al.* [ATLAS Collaboration], Phys. Lett. B **763** (2016) 313
- [36] M. Alvioli and M. Strikman, Phys. Rev. C **100** (2019) no.2, 024912
- [37] C. M. Tarbert *et al.*, Phys. Rev. Lett. **112** (2014) no.24, 242502
- [38] M. Warda, X. Vinas, X. Roca-Maza and M. Centelles, Phys. Rev. C **81** (2010) 054309
- [39] B. Blok and M. Strikman, Phys. Lett. B **772** (2017) 219
- [40] M. L. Mangano, M. Moretti, F. Piccinini, R. Pittau and A. D. Polosa, JHEP **0307** (2003) 001
- [41] J. Pumplin *et al.*, JHEP **0207** (2002) 012
- [42] K. J. Eskola, H. Paukkunen and C. A. Salgado, JHEP **0904** (2009) 065
- [43] S. Chatrchyan *et al.* [CMS Collaboration], Phys. Rev. D **89** (2014) no.9, 092010
- [44] V. Khachatryan *et al.* [CMS Collaboration], Phys. Rev. D **94** (2016) no.11, 112005
- [45] M. Aaboud *et al.* [ATLAS Collaboration], JHEP **1611** (2016) 110
- [46] P. Gunnellini, doi:10.1007/978-3-319-22213-4, 10.3204/DESY-THESIS-2015-010
- [47] Z. Bern *et al.*, Phys. Rev. Lett. **109** (2012) 042001
- [48] S. Badger, B. Biedermann, P. Uwer and V. Yundin, Phys. Lett. B **718** (2013) 965
- [49] D. Binosi, J. Collins, C. Kaufhold and L. Theussl, Comput. Phys. Commun. **180** (2009) 1709